

Spontaneous Parametric Downconversion and Proof of the Existence of Photons

Ryan LaRose

Winter 2017

Abstract

Two experiments in quantum mechanics are performed: spontaneous parametric downconversion and proof of single photon existence. In the former, we achieve coupled photon states and verify a Gaussian distribution of photon count rate vs. detector angle. In the latter, with a three detector assembly we measure the degree of second order coherence $g^{(2)}(0) = 0.0404 \pm 0.1368$ and thereby experimentally demonstrate the existence of photons. By performing a two detector measurement, we reaffirm the classical prediction of $g^{(2)}(0) \geq 1$ and regain the wave nature of light. In addition, other possible experiments that could be performed with a similar experimental setup, such as quantum entanglement and local realism, are discussed.

1 Introduction

This paper presents two experiments important to the foundation of quantum mechanics and whose results have important implications for modern technological research and applications. The first experiment, spontaneous parametric downconversion, explores the process of converting a photon into two coupled photons of lower energy. The second seeks to experimentally prove the existence of photons. An optical table equipped with a 805 nm laser, three half wave plates, a birefringent BBO crystal, several photon detectors, and a coincidence counting unit form the bulk of the equipment. Both experiments performed are based off those included in Beck's *Quantum Mechanics: Theory and Experiment* [2]. Additionally, we describe other possible experiments that could be performed with this same experimental setup.

2 Experimental Setup

Each experiment uses essentially the same equipment and configuration but performs different measurements. This section discusses the general experimental equipment and its operation, and ore specific details are included in each subsequent section. An overhead view of the optics table is shown in Figure 1.

Highlighted in red are the fundamental components. The laser emits a beam of photons at 405 nm. The green cylindrical guides surround the beam and prevent anything—a hand, arm, or shiny surface—from entering the beam path. Two mirror assemblies reflect the beam and ensure consistent polarization. Once the photons deflect off the second mirror at B, they are sent through a half wave plate—the “pump” half wave plate and subsequently, at C, the beam travels through the β -Barium Borate (BBO). This is where the spontaneous parametric downconversion process occurs and produces two separate beams, separated by an approximate angle of three degrees. Both of these beams are then sent to the detection assembly.

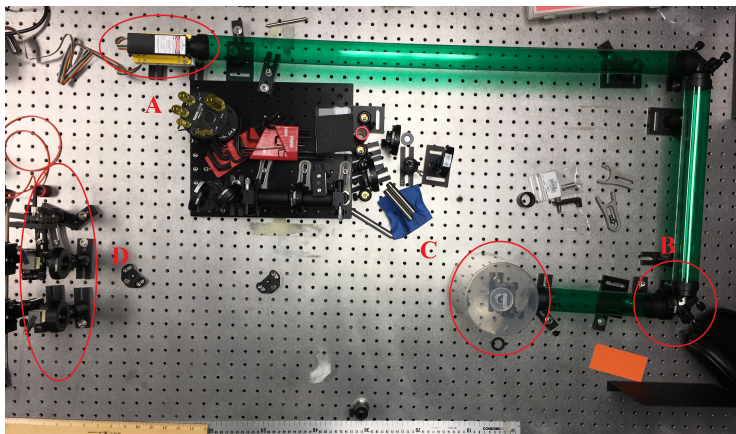


Figure 1: A picture of the experimental equipment. A: The laser. B: The pump half wave plate. C: Downconversion crystal. D: Detection assembly (See Figure 2).

At the detection assembly (see Figure 2), the photons are sent through a half wave plate and then a 50/50 beam splitter. (This occurs for both beams resulting from SPDC process.) Only one detector measures both beams from the beam splitter—these are termed the B and B' photons and detectors. The other is referred to as the A detector. These three beams are then guided via fiber optics to a system of electronics, the most important component of which being the coincidence counting unit (CCU). An RG780 filter ensures that no stray light from the pump enters the CCU. This device determines when photons from any combination of A , B , and B' are coincident—ie, occurring at the same time. This signal is then sent to a computer running LabPro.vi software and is the primary source of measurement for the experiments. When measurements are being taken, all stray room light is blocked out by thick black curtains. A green lamp, which is blocked by the RG780 filter and not picked up by the CCU, is used to provide enough visibility.

3 Spontaneous Parametric Downconversion

Much of the experimentation requires correctly aligning the optical components. Once this is done, each experiment is essentially just a different measurement performed on the computer. The first task is to properly align the pump beam and position the resulting detectors such that the two beams from SPDC are also aligned.

All subsequent experiments rely on photon pairs produced via spontaneous parametric downconversion, so it is essential to have this properly configured. SPDC is simply a process in which light of one frequency is converted into light of a different frequency [2]. The input wave is termed the pump (at angular frequency ω_p), and the two outputs are called the signal and idler (ω_s and ω_i , respectively). This inefficient process occurs inside the nonlinear BBO crystal shown in Figure 1. It is important to note that energy conservation requires the energy of the pump photon to be equal to the sum of the signal and idler photon energies:

$$\hbar\omega_p = \hbar\omega_s + \hbar\omega_i \iff \omega_p = \omega_s + \omega_i. \quad (1)$$

Additionally, conservation of momentum requires that

$$\hbar\mathbf{k}_p = \hbar\mathbf{k}_s + \hbar\mathbf{k}_i \iff \mathbf{k}_p = \mathbf{k}_s + \mathbf{k}_i. \quad (2)$$

Our setup is configured such that $\omega_p = 810$ nm and $\omega_s = \omega_i = 405$ nm.

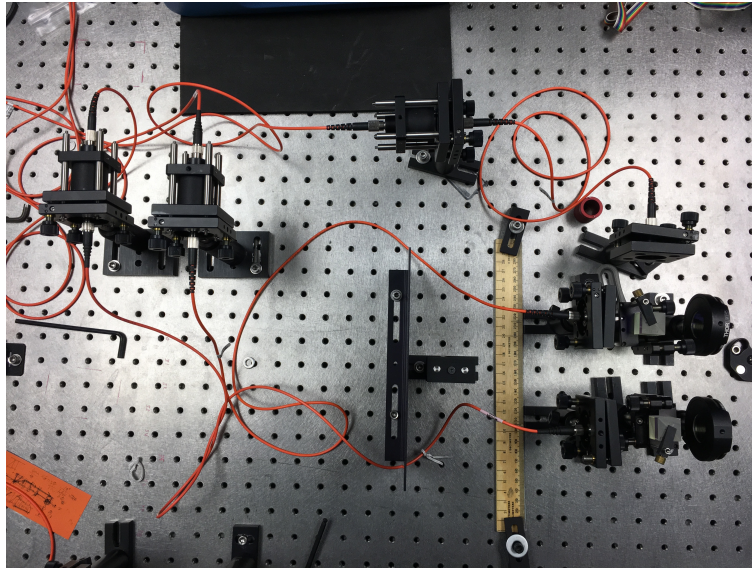


Figure 2: An overhead picture of the detection assembly consisting of half wave plates, beam splitters, and fiber optic cables. In this orientation, the beam enters the detectors at the right and travels to the left in the image. The coincidence counting unit (not pictured) is positioned just beyond the RG780 filters in the upper left of this image.

A complete description of the alignment procedures can be found in [2] and [1]. Without getting too detailed, the mirrors that reflect the beam pump are first aligned such that the pump hits the center of the BBO crystal. Then, the horizontal and vertical tilt of the crystal stand are varied to ensure optimal SPDC. Using Snell’s Law and the known frequencies of the signal and idler beams, the correct geometry of the A and B detectors is determined and established. The tilt of these detectors is then varied, and then the position and angle of the beam splitters is aligned. Lastly, the B' detector position and tilt are aligned.

For this process, a coarse alignment is generally done with a standard HeNe laser attached to the fiber optic coupler. (This coupler is what the fiber optics from the detectors feed into. By replacing this with the HeNe fiber optic, a visible beam is projected back through the optical system.) After the coarse alignment, the laser is powered on and a fine alignment is done by maximizing the photon counts displayed in the software.

To explore how the count rate depends upon the optimal angle, we first determine the position of the detector that produces the maximal counts. This position is recorded on a fixed ruler on the optical table running perpendicular to the detector assembly. The position is then converted to an angle through elementary geometry, and we then vary the angle of the detector by 0.1° and record the count rates. The results are shown in Figure 3.

As expected, the distribution follows (roughly) a Gaussian profile of the form

$$y(\theta) = a + be^{-\theta^2/\sigma^2}. \quad (3)$$

Using standard nonlinear fitting procedures¹, we find the fit parameters to be $a = 5.486$, $b = 502.898$, and $\sigma = 0.264$. This small width of the beam shows that it is crucial to have the detectors in the optimal position for recording counts. Just two tenths of a degree in either direction results in about half the count rates!

¹The fitting process was done using *Solver* in Excel.

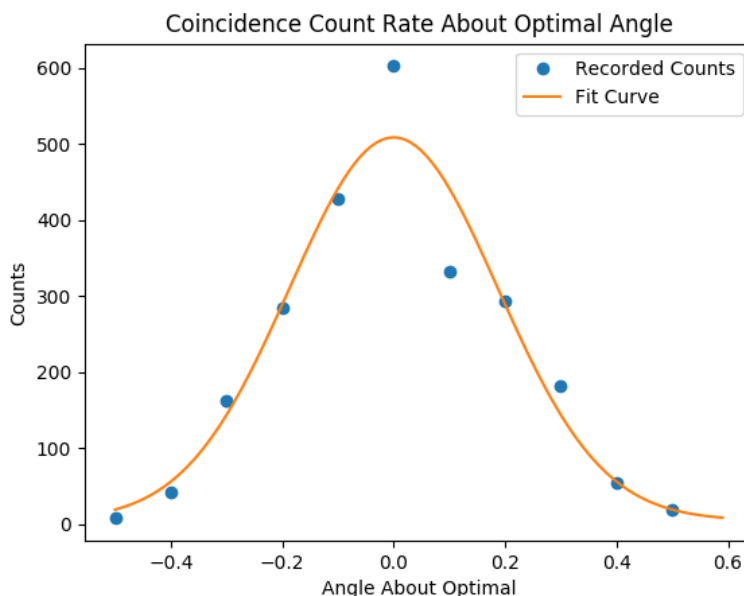


Figure 3: A graph of our recorded count rates as a function of angle about the optimal position.

4 Proof of the Existence of Photons

Introduction The purpose of this experiment is to demonstrate, or “prove,” that photons exist. Classically, light is solely an electromagnetic wave; quantum mechanically, light has both wave-like and particle-like behavior. To prove light is made of photons, we perform measurements—to be subsequently described—that cannot be explained by the classical wave theory of light.

This is somewhat tricky because the detection of light is always done electronically and is discrete due to the inherent discrete nature of electrons. Observing granularity in the measurement of a field is necessary to prove the existence of photons, but it is not sufficient. Because photons do not exist in classical physics, an experiment that requires photons to explain its results means there is more to light than solely a wave. If our measurement cannot be explained solely by classical waves, then we regard this as proof of the existence of photons.

The parameter that we will measure is the degree of second order coherence, $g^{(2)}(0)$. A detailed account of this parameter can be found in [2] and [3]. Here, we include a brief discussion of the classical and quantum calculations. Simply put, $g^{(2)}(0)$ measures the correlations between simultaneous measurements of intensities. Classically, if τ is the time delay between the intensity measurements, the correlation between the intensity of I_B and $I_{B'}$ at time t is given by

$$g_{B,B'}^{(2)}(\tau) = \frac{\langle I_B(t+\tau)I_{B'}(t) \rangle}{\langle I_B(t+\tau) \rangle \langle I_{B'}(t) \rangle}$$

For simultaneous measurements, τ is set to zero, and by using relationships between reflected and transmitted intensities $I_B = TI_I$ and $I_{B'} = RI_I$, where I_I is the intensity of the incident beam, it can be shown that

$$g_{B,B'}^{(2)}(0) = g^{(2)}(0) = \frac{\langle [I_I(t)]^2 \rangle}{\langle I_I(t) \rangle^2}.$$

By the Cauchy-Schwartz inequality, it thus follows immediately that

$$g^{(2)}(0) \geq 1 \quad \text{for classical fields} \quad (4)$$

The same can be shown for semi-classical fields (see [2]). Without going through the calculation for the quantum case (see [3] or [4]), we note that *if we measure $g^{(2)}(0) < 1$, the result cannot be explained classically. Hence, photons exist.*

Procedure We use the same setup described in detail in Section 2. A very large part of the experiment is aligning all detectors and finding the correct polarization state—ie, the angle of the pump half wave plate (HWP), the A HWP, and the B/B' HWP—to maximize the count rates on the A , B , and B' detectors. (An algorithmic approach to doing so is described in the experimental writeup by Beck ([2]).) After first finding the optimal pump HWP angle, we then rotate the A half wave plate to maximize the counts there. As for the B/B' HWP, the matter is slightly more sensitive because the count rates on B and B' are inversely proportional—that is, as this wave plate is rotated, counts on B increase while counts on B' decrease, and vice versa. We found that the best statistics for $g^{(2)}(0)$ measurements were obtained by having roughly equal counts on the B and B' detectors.

Results It is relatively straightforward—but out of the scope of this paper—to compute $g^{(2)}(0)$ from detector counts. The relationship [4] is

$$g^{(2)}(0) = \frac{N_{ABB'}N_A}{N_{AB}N_{B'}}, \quad (5)$$

where N_A is the number of counts at detector A , etc. The same software used to record count rates computes the degree of second order coherence as per this formula. A sample screenshot for a trial is shown in Figure 4. This measurement was taken with an update period of $1.0 \mu\text{s}$. By update period, we mean the refresh rate of the software while integrating counts—an update period of $1.0 \mu\text{s}$ thus means the software records all counts between time t and $t+1.0 \mu\text{s}$ and uses this value in (5). Also shown in this screenshot are the ABB' coincidence window—the time interval that detections are considered to be coincident, or simultaneous—the number of “points”—ie, the number of one second time intervals taken in the entire measurement—and three plots showing various quantities over time—the most notable of which is the $g(2)$ plot in the bottom center, which shows the value of $g^{(2)}(0)$ over time. Adjacent to this graph, in the bottom right of the screen, are the current, average, and expected values of $g^{(2)}(0)$, along with its standard deviation. The “thermometers” along the top of the image show the count rates we obtained in taking this measurement.

For an update period of $1 \mu\text{s}$ with measurements taken over 1000 seconds ≈ 16 minutes, we obtain a value of

$$g^{(2)}(0) = 0.0404 \pm 0.1368. \quad (6)$$

Our average value is significantly lower than the classical requirement of being ≥ 1 . Indeed, our measurement is a little over seven standard deviations below the classical expectation. To confirm these findings, we take three additional measurements with different update periods—namely, 5, 10, and 20 μs . A table of results is shown in Figure 5.

The average value stays around 0.04 for each update period, but the standard deviation decreases notably as the update period increases. This is because we are obtaining more count rates and thus getting better statistics. In our final trial, our value of $g^{(2)}(0)$ is over 26 standard deviations from one. This is a clear violation of the classical requirement (4). As per our above argument, we take this as proof for the existence of photons.

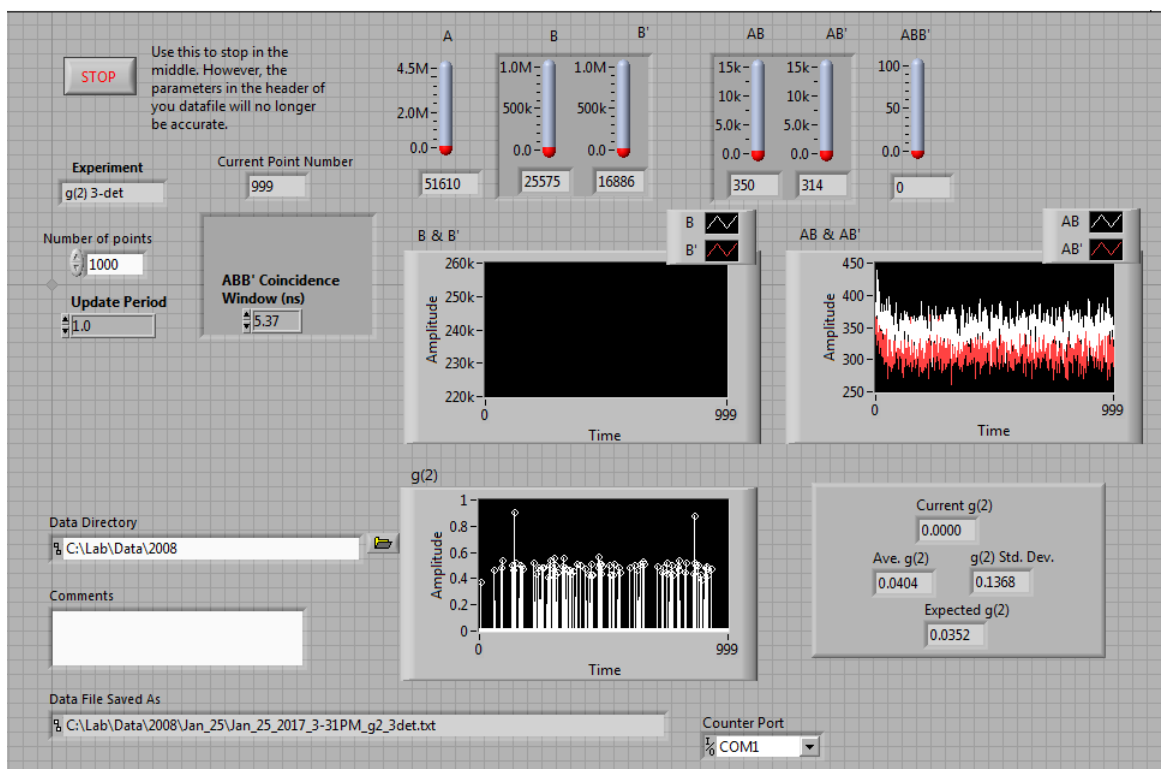


Figure 4: A screenshot of the labpro.vi software used in the proof of single photons experiment. An description of each graphic can be found in the “Results” subsection on page 5. The most important visual is the display of $g^{(2)}(0)$ in the lower right.

Update period (μs)	$\langle g^{(2)}(0) \rangle$	Std. Dev.	Std. Devs. from 1
1.0	0.0404	0.1368	7.01
5.0	0.0463	0.0657	8.17
10.0	0.0476	0.0417	22.84
20.0	0.0490	0.0356	26.71

Figure 5: Results of measuring the degree of second order coherence over four trials of different update periods. For each, measurements were taken over a period of 1000 seconds, or about 16 minutes.

4.1 Seeing the Wave Nature of Light

The crucial aspect of the preceding experiment is the three detector measurement, the third detector being A . When we get a count at A , we know immediately via the SPDC process that there is a coupled, single photon at the B/B' detector assembly. Conditioning the counts at B and/or B' on measurements at A thus guarantees we only take measurements of single photons, from which the quantum mechanical prediction comes into play. However, if we relax this condition and move to a two-detector measurement (B and B'), there is nothing to guarantee a single photon at the detectors. In other words, we should not expect the classical requirement (4) to be violated.

Interestingly enough, this is indeed what we see. A portion of the labpro.vi software showing our results is shown below.

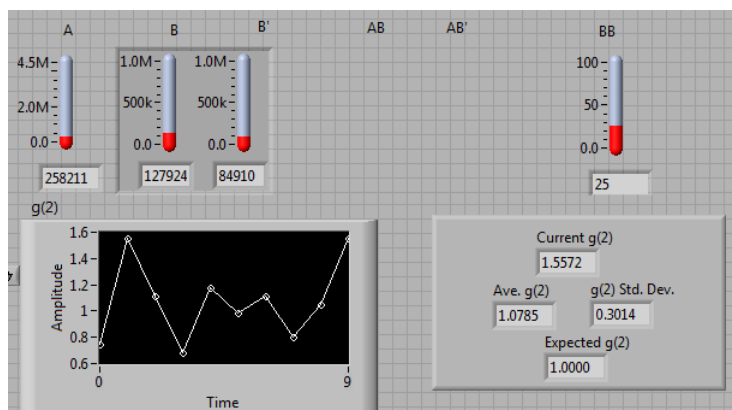


Figure 6: A picture of the software showing our results for a two detector measurement of $g^{(2)}(0)$, which reaffirms the wave nature of light.

With a value of

$$g^{(2)}(0) = 1.0785 \pm 0.3014, \quad (\text{two detector measurement}) \quad (7)$$

our average value is much greater than the previous three detector results of around 0.04. This trial was taken with an update period of $20 \mu\text{s}$, but for only ten seconds (due to time constraints). Our large standard deviation is likely due to the short data collection interval. However, it is easy to see the stark difference in values just by turning off, so to speak, the A detector, and the fact that our average corroborates the classical prediction (4) reaffirms the wave nature of light.

5 Other Fundamental Experiments in Quantum Mechanics

With this same experimental configuration, it is possible to explore other seminal experiments whose results have important implications for quantum mechanics and many applications, such as quantum information science and quantum computing. Due to time constraints, we were only able to successfully perform the spontaneous parametric downconversion and proof of photon existence experiments. One other possible experiment, outlined carefully in [2], is testing local realism.

A system is *local* if measurements performed in one place can affect the outcome of measurements performed somewhere else, and *realism* refers to the notion that objects have measurable quantities, whether we measure them or not. The goal of this experiment is to demonstrate that quantum systems are not confined by local realism. This is done, briefly put, by rotating half wave plates until the Bell state

$$|\psi\rangle = \sqrt{a}|H\rangle_a|H\rangle_B + \sqrt{1-a}e^{i\phi}|V\rangle_A|V\rangle_B \quad (8)$$

where $|H\rangle$ and $|V\rangle$ are basis states (horizontal and vertical, respectively), ϕ is the relative phase between pump beam and the beam after the downconversion crystal, and a is the ratio of the probability of the production of horizontally or vertically polarized photon pairs, which is controlled experimentally. Once this state is obtained, one can test the Bell-Clauser-Horne inequality $H \leq 0$, where

$$H \equiv P(\beta, \beta) - P(-\alpha, \alpha) + P(\beta, \alpha^\perp) + P(-\alpha^\perp, -\beta), \quad (9)$$

where $\alpha^\perp = \alpha \pm \pi/4$ and α, β are angles (dependent on the experimental setup, see [2]) of the wave plates in front of detectors A, B . Lastly, $P(\theta_A, \theta_B)$ is the joint probability that photons polarized

along these directions will be measured,

$$P(\theta_A, \theta_B) \equiv \frac{N_{AB}}{N_{AB} + N_{AB'} + N_{A'B} + N_{A'B'}}. \quad (10)$$

Ideally, four detectors would be available to perform this experiment (the fourth being A' , playing the role of B' at the A detector assembly). However, it is possible (though more time consuming) to perform the test with three detectors by rotating the A detector by $\pi/8$, which properly rotates the incoming polarization and achieves the same effect as an A' detector. The only downside is that twice as many trials need to be performed.

As mentioned, we were not able to complete this experiment due to time constraints and not being able to properly produce the Bell state (8). Once this state is achieved, it is simply a matter of recording the four count rates N_{AB} , $N_{AB'}$, $N_{A'B}$, and $N_{A'B'}$ and calculating the probability via (10) for each of the four configurations in (9).

In addition to testing local realism, it is also possible to perform experiments on single photon interference and measurement of quantum states. We do not describe these here but note that they are included in [2].

6 Conclusions

In the SPDC experiment, we successfully aligned the optics and birefringent crystal to obtain coupled photons at the A and B detectors. By first finding the optimal angle of the detectors, we showed experimentally that the photon count rate follows a Gaussian distribution about this optimal angle, as anticipated. The minimal width of this curve demonstrates the importance of having detectors in the correct position for successful measurements and good statistics in following experiments.

In the single photon experiment, we showed that the classical prediction of $g^{(2)}(0) \geq 1$ was statistically violated for the three detector measurement, thereby proving granularity exists in the photon field. By removing the A detector and performing only two detector measurements of the degree of second order coherence, we showed that light does satisfy the classical prediction and thus has wave nature. For the former measurement, we measured $g^{(2)}(0)$ to be a maximum of around 27 standard deviations below one. Although this is certainly a statistically significant result, other experimenters [3] have achieved measurements as good as 100 standard deviations below one.

References

- [1] Sih, Vanessa, “Spontaneous Parametric Downconversion and Proof of the Existence of Photons,” March 2014, University of Michigan Department of Physics, Ann Arbor, MI
- [2] Beck, Mark, *Quantum Mechanics: Theory and Experiment*, 2012, Oxford University Press, New York, NY
- [3] Thorn, J.J. *et al.*, “Observing the Quantum Behavior of Light in an Undergraduate Laboratory,” September 2004, American Journal of Physics, Vol. 72, No. 9
- [4] Beck, Mark, “Comparing Measurements of $g^{(2)}(0)$ Performed with Different Coincidence Detection Techniques,” August 2007, Whitman College Department of Physics, Walla Walla, WA